

Measurement of the Diffractive Deep-Inelastic Scattering Cross Section with a Leading Proton at HERA

Mikhail Kapishin (for the H1 Collaboration) *

JINR, Dubna, Russia

E-mail: kapishin@mail.desy.de

Results are reported on a new measurement of the cross section for diffractive deep-inelastic scattering process $ep \rightarrow eXp$ with the leading final state proton detected in the H1 Forward Proton Spectrometer, using data collected at HERA-2. The cross section dependences on the proton fractional longitudinal momentum loss x_p and the squared four-momentum transfer at the proton vertex are interpreted in terms of an effective pomeron trajectory and a sub-leading exchange. The hypothesis of proton vertex factorisation is tested. The ratio of the diffractive to the inclusive ep cross section is studied. The data are compared to QCD predictions at next-to-leading order based on parton distribution functions previously extracted from measurements of diffractive and inclusive deep-inelastic scattering.

XVIII International Workshop on Deep-Inelastic Scattering and Related Subjects, DIS 2010

April 19-23, 2010

Firenze, Italy

*Speaker.

1. Introduction

Diffractive processes such as $ep \rightarrow eXp$ have been studied extensively in deep-inelastic electron-proton scattering (DIS) at the HERA collider [1–4]. Their understanding at fundamental level is crucial for the development of quantum chromodynamics (QCD) at high parton densities. In a number of previous analyses, including [2], diffractive DIS events were selected on the basis of the presence of a large rapidity gap (LRG) between the leading proton and the remainder of the hadronic final state X . A complementary way to study diffractive processes is by direct measurement of the outgoing proton using Forward Proton Spectrometers (FPS) [1, 3]. In contrast to the LRG case, the squared four-momentum transfer at the proton vertex t can be reconstructed. The FPS also allows measurements up to higher values of the proton fractional longitudinal momentum loss x_P than is possible with the LRG method, extending into regions where the sub-leading trajectory is the dominant exchange. The FPS measurements provide a means of testing in detail whether the variables x_P and t associated with the proton vertex can be factorised from the variables $\beta = x/x_P$ and Q^2 describing the hard interaction with the photon. Here β is the longitudinal momentum fraction of the colour singlet carried by the struck quark, x is the Bjorken scaling variable.

2. The reduced cross section $\sigma_r^{D(4)}$ and test of proton vertex factorisation

In this report, a new measurement of the reduced cross section $\sigma_r^{D(4)}(\beta, Q^2, x_P, t)$ for the diffractive DIS process $ep \rightarrow eXp$ is presented, using the FPS data collected with the H1 detector at HERA-2. The reduced cross section is related to the diffractive structure functions $F_2^{D(4)}$ and $F_L^{D(4)}$ by

$$\sigma_r^{D(4)} = F_2^{D(4)} - \frac{y^2}{1+(1-y)^2} F_L^{D(4)},$$

where y is the inelasticity. The reduced cross section is equal to the diffractive structure function $F_2^{D(4)}(\beta, Q^2, x_P, t)$ to good approximation in the relatively low y region covered by the current analysis. The analysed data sample corresponds to an integrated luminosity of 156 pb^{-1} . The data cover the range $0.1 < |t| < 0.7 \text{ GeV}^2$, $x_P < 0.1$, $4 < Q^2 < 110 \text{ GeV}^2$ and $0.001 < \beta < 1$. The statistics of DIS

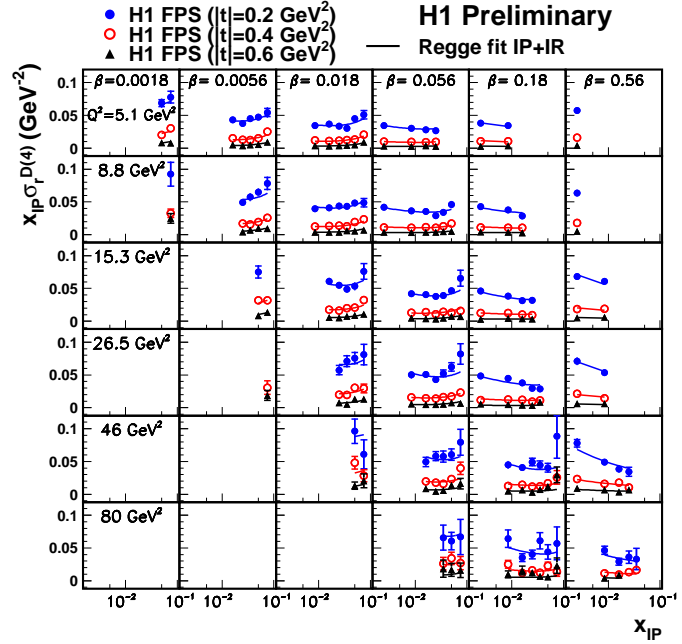


Figure 1: The diffractive reduced cross section, shown as a function of x_P for different values of t , β and Q^2 . The solid curves represent the results of the phenomenological ‘Regge’ fit to the data, including both pomeron (IP) and sub-leading (IR) trajectory exchange.

41 events with a leading proton are increased by a factor 20 compared to the previous H1 FPS anal-
 42 ysis [1]. The kinematic range of the FPS measurement is extended to higher Q^2 . Figure 1 shows
 43 $x_{\mathbb{P}} \sigma_r^{D(4)}$ as a function of $x_{\mathbb{P}}$ for different t , β and Q^2 values. To describe the $x_{\mathbb{P}}$ and t dependences
 44 quantitatively, the structure function $F_2^{D(4)}$ is parameterised by the form

$$45 \quad F_2^{D(4)} = f_{\mathbb{P}}(x_{\mathbb{P}}, t) \cdot F_{\mathbb{P}}(\beta, Q^2) + n_{\mathbb{R}} \cdot f_{\mathbb{R}}(x_{\mathbb{P}}, t) \cdot F_{\mathbb{R}}(\beta, Q^2) ; \quad f_{\mathbb{P},\mathbb{R}}(x_{\mathbb{P}}, t) = A_{\mathbb{P},\mathbb{R}} \cdot \frac{e^{B_{\mathbb{P},\mathbb{R}} t}}{x_{\mathbb{P}}^{2\alpha_{\mathbb{P},\mathbb{R}}(t)-1}} ,
 46$$

47
 48 which assumes a separate proton vertex factorisation of the $x_{\mathbb{P}}$ and t dependences from those on
 49 β and Q^2 for both the pomeron and a sub-leading exchange with no interference between the
 50 two contributions. The factors $f_{\mathbb{P}}$ and $f_{\mathbb{R}}$ correspond to flux factors for the exchanges and are taken
 51 from the Regge-motivated functions. The free parameters of the fit are the intercept and slope of the
 52 pomeron trajectory, $\alpha_{\mathbb{P}}(t) = \alpha_{\mathbb{P}}(0) + \alpha'_{\mathbb{P}} t$, the exponential t -slope parameter $B_{\mathbb{P}}$, the normalisation
 53 coefficients $F_{\mathbb{P}}(\beta, Q^2)$ for the pomeron contribution at each of the (β, Q^2) values considered, and
 54 the single parameter $n_{\mathbb{R}}$ describing the normalisation of the sub-leading exchange contribution. As
 55 in [1, 2], the normalisation coefficients $F_{\mathbb{R}}(\beta, Q^2)$ for the sub-leading exchange in each β and Q^2
 56 bin are taken from a parameterisation of the pion structure function [8].

57 The fit provides a good description of the $x_{\mathbb{P}}$ and t dependences of the data. The result for
 58 $\alpha_{\mathbb{P}}(0) \simeq 1.10$ (figure 2) is compatible with that obtained from H1 data previously measured using
 59 the LRG and FPS methods [1, 2] and with ZEUS measurements [3, 4]. It is also consistent within
 60 uncertainties with the pomeron intercept describing soft hadronic scattering, $\alpha_{\mathbb{P}}(0) \simeq 1.08$ [6].

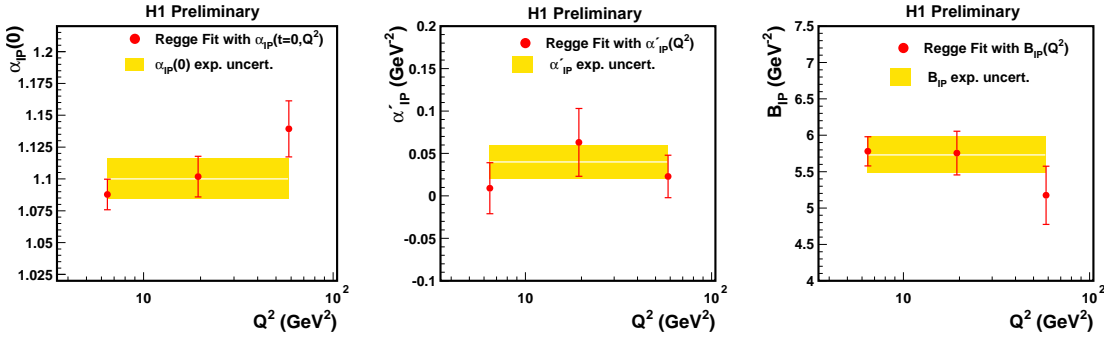


Figure 2: Results from the ‘Regge’ fit in which additional free parameters are included, corresponding to the values of $\alpha_{\mathbb{P}}(0)$, $\alpha'_{\mathbb{P}}$ and $B_{\mathbb{P}}$ in three different ranges of Q^2 . The bands show the result and experimental uncertainty from the standard fit over the whole Q^2 range.

61 In a Regge approach with a single linear exchanged pomeron trajectory, $\alpha_{\mathbb{P}}(t) = \alpha_{\mathbb{P}}(0) + \alpha'_{\mathbb{P}} t$, the
 62 exponential t -slope parameter B of the diffractive cross section is expected to decrease logarithmi-
 63 cally with increasing $x_{\mathbb{P}}$, an effect which is often referred to as ‘shrinkage’ of the diffractive peak.
 64 The degree of shrinkage depends on the slope of the pomeron trajectory, which is $\alpha'_{\mathbb{P}} \simeq 0.25 \text{ GeV}^{-2}$
 65 for soft hadron-hadron scattering at high energies. The FPS data favour a small value of $\alpha'_{\mathbb{P}}$ (fig-
 66 ure 2), as expected in perturbative models of the pomeron [7]. This result is inconsistent with the
 67 expected value of $\alpha'_{\mathbb{P}}$ from soft hadron-hadron scattering. The results for $\alpha'_{\mathbb{P}}$ and $B_{\mathbb{P}}$ are compat-
 68 ible with those obtained previously from the H1 and ZEUS data measured using the FPS detec-
 69 tors [1, 3]. To check a possible breakdown of proton vertex factorisation implied by a dependence
 70 of the $\alpha_{\mathbb{P}}(0)$, $\alpha'_{\mathbb{P}}$ and $B_{\mathbb{P}}$ on Q^2 , a modified version of the ‘Regge’ fit of the data is performed in

71 three different ranges of Q^2 . The results of the fits, shown in figure 2, indicate no strong dependence
 72 on Q^2 .

73 The t -dependence of the cross section
 74 is parameterised by an exponential function
 75 such that $d\sigma/dt \propto e^{Bt}$. Figure 3 shows the
 76 slope parameter B as a function of x_P for
 77 data averaged over Q^2 and β . The results
 78 for B are compared with a parameterisation
 79 of the t -dependence from the ‘Regge’ fit to
 80 $F_2^{D(4)}$. A good description of the data over
 81 the full x_P , Q^2 and β range in figure 3 con-
 82 firms the quality of the fit. At low x_P , the
 83 data are compatible with a constant slope pa-
 84 rameter, $B \simeq 6 \text{ GeV}^{-2}$. No significant Q^2
 85 or β dependence of the slope parameter B
 86 is observed for data points with $x_P \leq 0.025$.
 87 The sub-leading exchange contribution inte-
 88 grated over this kinematic range is 7%. A
 89 weak decrease of the slope B from 6 GeV^{-2}
 90 to below 5 GeV^{-2} is observed towards larger
 91 values of $x_P > 0.05$, where the contribution
 92 from the sub-leading exchange is significant
 93 This reduction of the slope parameter indi-
 94 cates that the size of the interaction region reduces for \mathbb{R} exchange compared to \mathbb{P} .

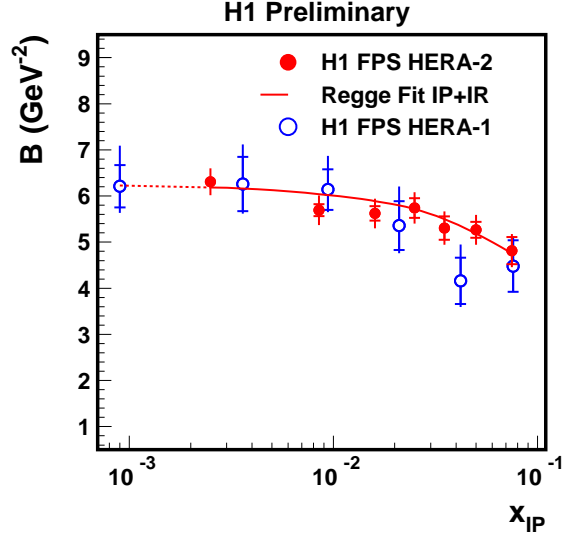


Figure 3: The slope parameter B obtained from the fit of the form $d\sigma/dt \propto e^{Bt}$ shown as a function of x_P . The data are averaged over Q^2 and β . The solid curve represents the results of the phenomenological ‘Regge’ fit to the data, including both pomeron (\mathbb{P}) and sub-leading (\mathbb{R}) trajectory exchange. The previously published H1 FPS results [1] are also shown.

95 3. Comparison between Diffractive and Inclusive DIS

96 By analogy with hadronic scattering, the diffractive and the total cross sections can be related
 97 via the generalisation of the optical theorem to virtual photon scattering [9]. Many models of
 98 low x DIS assume links between these quantities [10, 11]. Comparing the Q^2 and x dynamics
 99 of the diffractive with the inclusive cross section is therefore a powerful means of developing
 100 our understanding of high energy QCD, comparing the properties of diffractive PDFs with their
 101 inclusive counterparts and testing models. Following [2], the evolution of the diffractive reduced
 102 cross section with Q^2 is compared with that of the inclusive DIS reduced cross section σ_r by
 103 forming the ratio $\sigma_r^{D(3)}(x_P, \beta, Q^2)/\sigma_r(x = \beta x_P, Q^2)$ multiplied by $(1 - \beta)x_P$ at fixed Q^2, β and
 104 x_P , using a parameterisation of the σ_r data from [5]. The diffractive reduced cross section is
 105 integrated over $|t| < 1 \text{ GeV}^2$. The ratio of the diffractive to the inclusive cross section is indeed
 106 approximately constant with β at fixed Q^2 except at large values of x_P where the sub-leading
 107 exchange contribution to the diffractive cross section is not negligible. In models in which both
 108 the diffractive and the inclusive cross sections are governed by a universal pomeron [10, 11], the
 109 remaining β and x_P dependences of the ratio arises due to the deviations from unity of the pomeron
 110 trajectory and the contribution of the sub-leading trajectory.

In order to compare the Q^2 dependences of the diffractive and the inclusive cross sections quantitatively, the derivative of their ratio with $\ln Q^2$ is extracted through fits of the form

$$(1 - \beta)x_P \sigma_r^{D(3)}(x_P, \beta, Q^2) / \sigma_r(x = \beta x_P, Q^2) = a_r(\beta, x_P) + b_r(\beta, x_P) \cdot \ln Q^2$$

The resulting values of b_r are shown in figure 4. The ratio of the diffractive to the inclusive cross section depends only weakly on Q^2 for most β and x_P values (the logarithmic derivative of the ratio, b_r , is consistent with zero within 1.5σ of the experimental uncertainties). Whereas the diffractive and inclusive reduced cross sections are closely related to their respective quark densities, the $\ln Q^2$ derivatives are approximately proportional to the relevant gluon densities in regions where the Q^2 evolution is dominated by the $g \rightarrow \bar{q}q$ splitting. The compatibility of b_r with zero thus implies that the ratio of the quark to the gluon density is similar in the diffractive and inclusive cases when considered at the same low x values. Proton PDF predictions reproduce the behaviour of the $\ln Q^2$ derivative of the ratio with β .

References

- [1] H1 Collaboration, Eur. Phys. J. C **48** (2006) 749
- [2] H1 Collaboration, Eur. Phys. J. C **48** (2006) 715
- [3] ZEUS Collaboration, Nucl. Phys. B **816** (2009) 1 [hep-ex/0408009].
- [4] ZEUS Collaboration, Nucl. Phys. B **800** (2008) 1
- [5] H1 Collaboration, Eur. Phys. J. C **64** (2009) 561 [arxiv:0904.3513]
- [6] G. Jaroszkiewicz and P. Landshoff, Phys. Rev. D **10** (1974) 170.
- [7] J. Bartels and H. Kowalski, Eur. Phys. J. C **19** (2001) 693 [hep-ph/0010345].
- [8] J. Owens, Phys. Rev. D **30** (1984) 943.
- [9] A. Mueller, Phys. Rev. D **2** (1970) 2963.
- [10] K. Golec-Biernat and M. Wüsthoff, Phys. Rev. D **59** (1999) 014017 [hep-ph/9807513].
- [11] J. Bartels, K. Golec-Biernat and H. Kowalski, Phys. Rev. D **66** (2002) 014001 [hep-ph/0203258].

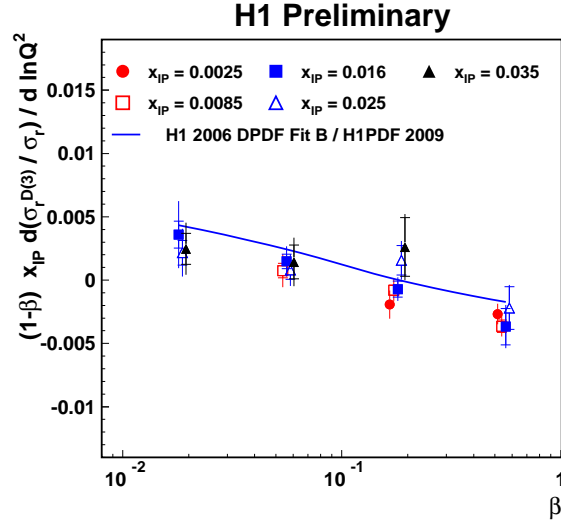


Figure 4: The logarithmic Q^2 derivative of the ratio of the diffractive reduced cross section $\sigma_r^{D(3)}(\beta, Q^2, x_P)$ to the inclusive reduced cross section $\sigma_r(x = \beta x_P, Q^2)$ multiplied by $(1 - \beta)x_P$, shown at different fixed values of x_P and β . The solid curve represents the results for the ratio of diffractive to inclusive PDF predictions [2, 5].